Radio Science, Volume 10, Number 12, pages 1055-1061, December 1975

Frequency and spatial correlation functions in a fading communication channel through the ionosphere

C. H. Liu and K. C. Yeh

Department of Electrical Engineering, University of Illinois at Urbana-Champaign, Urbana, Illinois 61801

(Received June 24, 1975.)

Equations for the two-frequency two-position mutual coherence functions are derived under the usual parabolic and Markov approximations. These equations are then solved numerically. It is shown that the mutual coherence functions occur naturally in the study of pulse distortion through a random communication channel and in the investigation of signal correlations. Contour plots of correlation functions show the possibility of having equal values at two frequency separations for a given spatial separation. This behavior is explainable in terms of overlapping Fresnel zones.

1. INTRODUCTION

Recently it has been observed that radio signals from communication satellites at a frequency as high as several GHz may experience the scintillation phenomenon when received on the ground [*Pope and Fritz*, 1971; *Skinner et al.*, 1971; *Sessions*, 1972; *Craft and Westerlund*, 1972; *Taur*, 1973]. This came as a surprise since scintillation was not anticipated to occur at such a high frequency. After some experimentation it is now believed that the scintillation is caused by the electron density irregularities in the ionosphere. As is well known, for a given electron density fluctuation, the rms fluctuation in the refractive index of the ionospheric medium is inversely proportional to the square of the signal frequency. Therefore, under conditions when GHz scintillation occurs, signals with a lower frequency will experience even more severe fading. This implies that the effects of multiple scattering on signal statistics are very important under such conditions. To obtain their statistics correctly, it is desirable to develop a scintillation theory that takes into account the multiple scattering effects. Thanks to the recent advances in the theory of wave propagation in random media, it is now possible to develop such a theory [*Liu et al.*, 1974*a*; *Yeh et al.*, 1975]. In this paper, we shall apply a similar technique to investigate the frequency and spatial correlations of signals passing through the irregularity slab. In satellite communications the ability to transmit wideband data is limited primarily by the inter-symbol interference which is closely related to the frequency correlation of the signal. On the other hand, information about the frequency and spatial correlation of the signal is essential in designing and analyzing frequency and/or spatial diversity schemes.

The problem is formulated in section 2, where equations for the mutual coherence functions used in the computation are derived. In section 3, numerical results are presented with discussions based on scattering theory and ionospheric physics. Some conclusions are made in section 4.

2. THE TWO-FREQUENCY MUTUAL COHERENCE FUNCTIONS

The geometry of the problem is shown in Figure 1. A slab of random electron density irregularities with thickness L is present in the ionosphere. The slab is characterized by the dielectric permittivity

$$\epsilon(\vec{r}) = \langle\epsilon\rangle[1 + \epsilon_1(\vec{r})]\epsilon_0 \tag{1}$$

where

$$\langle\epsilon\rangle = (1 - \omega_p^2/\omega^2) \tag{2}$$

$$\epsilon_1(\vec{r}) = -\frac{(\omega_p^2/\omega^2)}{1 - \omega_p^2/\omega^2}\left[\frac{\Delta N(\vec{r})}{N_0(z)}\right] \tag{3}$$

and $\omega_p^2 = e^2 N_0(z)/m\epsilon_0$ is the square of the angular electron plasma frequency of the background ionosphere. ϵ_0 is the vacuum permittivity, e and m are the charge and mass of electrons respectively. The background electron density $N_0(z)$ is a function of height with a typical scale height H. The percentage electron density fluctuation $\Delta N(\vec{r})/N_0(z)$ is assumed to be a homogeneous random field with

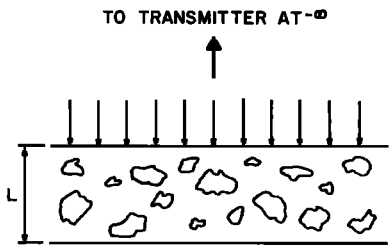

Fig. 1. Geometry of the problem.

a typical scale size l_0. In case of ionospheric propagation, the following inequality is usually satisfied:

$$H \gg l_0 \gg \lambda \tag{4}$$

where λ is the wavelength of the wave. This inequality implies that only forward scattering is important in the random scattering process [*Tatarski*, 1971] and the WKB solution is valid for the wave propagation [*Yeh and Liu*, 1972]. Let us assume a monochromatic wave propagating in the z direction in the medium. The field can be expressed as

$$E(\vec{r},t) = u(\vec{r},\omega)\exp\left(\left(j\omega\left\{t - \int^{z}[\langle\epsilon(\zeta)\rangle]^{1/2}\,d\zeta/c\right\}\right)\right) \tag{5}$$

with the complex amplitude $u(\vec{r},\omega)$ approximately satisfying the equation

$$-2jk\,\partial u/\partial z + \nabla^2 u + k^2\epsilon_1(\vec{r})\,u = 0 \tag{6}$$

where $k = \omega(\langle\epsilon\rangle)^{1/2}/c$. In deriving (6), the validity of the WKB solution is assumed and the depolarization effect has been neglected. If, instead of a monochromatic wave, a signal with Fourier amplitude $A(\omega)$ is incident on the irregularity slab, we can express this signal as it propagates through the medium as

$$p(\vec{r},t) = \int_{-\infty}^{+\infty} A(\omega)\,u(\vec{r},\omega)\exp\left(\left(j\omega\left\{t - \int^{z}[\langle\epsilon(\zeta)\rangle]^{1/2}\,d\zeta/c\right\}\right)\right)d\omega \tag{7}$$

In (7) we note that the effect of the background dispersive properties on the signal is contained mainly in the exponential factor while the effect due to random scattering is given by $u(\vec{r},\omega)$ which satisfies (6). The statistical properties of the signal p, such as rms intensity fluctuation, correlation, etc., are related to the statistical characteristics of the complex amplitude u. In particular, we shall be concentrating on the following two second-moment functions

$$\Gamma(\vec{\rho},z,\omega_1,\omega_2) = \langle u(\vec{\rho}_1,z,\omega_1)\,u^*(\vec{\rho}_2,z,\omega_2)\rangle \equiv \langle u_1\,u_2^*\rangle \tag{8}$$

$$\bar{\Gamma}(\vec{\rho},z,\omega_1,\omega_2) = \langle u(\vec{\rho}_1,z,\omega_1)\,u(\vec{\rho}_2,z,\omega_2)\rangle \equiv \langle u_1\,u_2\rangle \tag{9}$$

where $\vec{\rho}_i = (x_i,y_i)$, $i = 1$ or 2, is the transverse coordinate of the field point and $\vec{\rho} = \vec{\rho}_1 - \vec{\rho}_2$. We shall call Γ and $\bar{\Gamma}$ the symmetric and antisymmetric two-frequency mutual coherence functions, respectively.

Using Γ and $\bar{\Gamma}$, it is possible to derive the statistical characteristics of the signal $p(t)$. For example, the intensity of the pulse at a given receiving point can be expressed as

$$\langle p(t)p^*(t)\rangle = \int\int_{-\infty}^{+\infty} A(\omega_1)A^*(\omega_2)\,\Gamma(0,z,\omega_1,\omega_2)\cdot\exp\left(\left(j\omega_1\left\{t - \int^{z}[\langle\epsilon(\zeta)\rangle]^{1/2}\,d\zeta/c\right\} - j\omega_2\left\{t - \int^{z}[\langle\epsilon(\zeta)\rangle]^{1/2}\,d\zeta/c\right\}\right)\right)d\omega_1\,d\omega_2 \tag{10}$$

where the mutual coherence function appears naturally. In addition to its close relation to the signal statistics, the mutual coherence function also contains information about both the frequency and spatial correlations of the signal, information that is vital to the analysis of frequency and/or spatial diversity schemes for the satellite-earth communication links.

Starting from (6), under the so-called parabolic equation approximation and Markov assumption [*Tatarski*, 1971], it is possible to derive equations for the mutual coherence functions that take into account the effects of multiple scattering [*Liu et al.*, 1974*b*; *Lee*, 1974]. In terms of the ionospheric parameters, these equations can be written for the case of plane waves:

$$\frac{\partial \Gamma}{\partial z} + j\frac{k_2 - k_1}{2k_1 k_2}\nabla_T^2 \Gamma + \frac{k_p^4}{8}\left[\left(\frac{1}{k_1^2} + \frac{1}{k_2^2}\right) A_N(0) - \frac{2}{k_1 k_2} A_N(\vec{\rho})\right]\Gamma = 0 \tag{11}$$

$$\frac{\partial \bar{\Gamma}}{\partial z} + j\frac{k_1 + k_2}{2k_1 k_2}\nabla_T^2 \bar{\Gamma} + \frac{k_p^4}{8}\left[\left(\frac{1}{k_1^2} + \frac{1}{k_2^2}\right) A_N(0) + \frac{2}{k_1 k_2} A_N(\vec{\rho})\right]\bar{\Gamma} = 0 \tag{12}$$

where

$$k_p = \omega_p/c, \quad k_i = \omega_i[\langle \epsilon(\omega_i)\rangle]^{1/2}/c, \quad i = 1,2 \tag{13}$$

and

$$A_N(\vec{\rho}) = \int_{-\infty}^{+\infty} [\langle \Delta N(\vec{\rho}_1, z)\Delta N(\vec{\rho}_2, z)\rangle / N_0^2]\, dz \tag{14}$$

$$\nabla_T^2 = \partial^2/\partial x^2 + \partial^2/\partial y^2 \tag{15}$$

Equation 11 has been used to study the propagation of pulse trains in a turbulent plasma under weak scattering conditions [*Liu et al.*, 1974*b*]. Some approximate analytic solutions of (11) and (12) have been obtained recently [*Ulaszek et al.*, 1975]. *Erukhimov et al.* [1973] solved (11) numerically for some special cases. In this paper, we shall present some results by numerically solving (11) and (12) for typical ionospheric conditions. For numerical convenience, the equations are first transformed into dimensionless forms in terms of normalized coordinates

$$\xi = x/l_0, \quad \eta = y/l_0, \quad \zeta = z/k_0 l_0^2 \tag{16}$$

$$\omega_1 = \omega_0(1 - X), \quad \omega_2 = \omega_0(1 + X), \quad k_0 = \omega_0/c \tag{17}$$

(11) and (12) become, after the transformation,

$$\frac{\partial \Gamma_1}{\partial \zeta} + jB_1 \nabla_T^2 \Gamma_1 - [CG(\xi,\eta)/D]\Gamma_1 = 0 \tag{18}$$

$$\frac{\partial \Gamma_2}{\partial \zeta} + jB_2 \nabla_T^2 \Gamma_2 + [CG(\xi,\eta)/D]\Gamma_2 = 0 \tag{19}$$

where ∇_T^2 now stands for $\partial^2/\partial\xi^2 + \partial^2/\partial\eta^2$, and

$$C = (1/4)\, k_0^3 l_0^3 (\omega_p/\omega_0)^4 \langle (\Delta N/N_0)^2\rangle \tag{20}$$

$$G(\xi,\eta) = A_N(\xi,\eta)/l_0 \langle (\Delta N/N_0)^2\rangle \tag{21}$$

$$D = (1 - X^2)\alpha\beta \tag{22}$$

$$B_1 = [(\alpha + \beta)X + \beta - \alpha]/2D \tag{23}$$

$$B_2 = [\alpha + \beta + (\beta - \alpha)X]/2D \tag{24}$$

$$\alpha = [1 - (\omega_p/\omega_0)^2/(1 - X)^2]^{1/2} \tag{25}$$

$$\beta = [1 - (\omega_p/\omega_0)^2/(1 + X)^2]^{1/2} \tag{26}$$

The functions Γ_1 and Γ_2 in (18) and (19) are related to the mutual coherence functions by

$$\Gamma(\vec{\rho}, z, \omega_0, X) = \Gamma_1 \exp[-CG(0)B_3\zeta] \tag{27}$$

$$\bar{\Gamma}(\vec{\rho}, z, \omega_0, X) = \Gamma_2 \exp[-CG(0)B_3\zeta] \tag{28}$$

where

$$B_3 = [1 + X^2 - (\omega_p/\omega_0)^2]/\alpha\beta D(1 - X^2) \tag{29}$$

Referring to the geometry of Figure 1, (18) and (19) are solved numerically from $z = 0$ to $z = L$ through the irregularity slab. The mutual coherence functions Γ and $\bar{\Gamma}$ are then computed from (27) and (28) respectively. The values of Γ and $\bar{\Gamma}$ at $z = L$ are then used respectively as "initial" conditions for the equations

$$\partial\Gamma/\partial\zeta + jB_1\nabla_T^2\Gamma = 0, \quad \zeta > \zeta_0 \tag{30}$$

$$\partial\bar{\Gamma}/\partial\zeta + jB_2\nabla_T^2\bar{\Gamma} = 0, \quad \zeta > \zeta_0 \tag{31}$$

which are the equations for the mutual coherence functions for $z > L$ in the region below the irregularity slab. In (30) and (31), $\zeta_0 = L/k_0 l_0^2$.

In the next section we present the numerical results computed this way.

3. NUMERICAL RESULTS

In order to carry out our computations numerically, a model ionosphere has to be chosen first. Since our main concern here is to investigate the effects of the localized irregularity slab on the radio signal, the background ionosphere is assumed to have a constant profile within the slab. On the other hand, we have tried to include in the irregularity models some features which are believed to be realistic based on the recent in-situ measurements. These measurements indicate that the power spectrum for the irregularities follows a power-law dependence in wave number, that the electron density fluctuations can be as high as 20% or even higher, and that the irregularity slab may extend to several hundred kilometers [*Dyson*, 1969; *Rufenach*, 1972; *McClure and Hanson*, 1973; *Dyson et al.*, 1974].

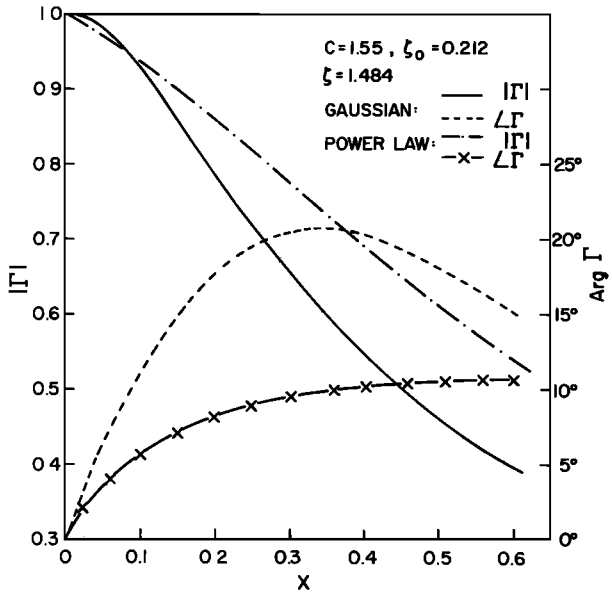

Fig. 2. Amplitude and phase of Γ as functions of frequency separation, for both power-law and gaussian spectra.

Consequently, in our computations, a power-law spectrum of the form

$$\Phi_N(\vec{K}) \propto 1/(1 + l_0^2 K^2)^2 \tag{32}$$

is assumed. For comparison, results are also obtained for a gaussian spectrum proportional to $\exp(-l_0^2 K^2)$.

Figure 2 shows $|\Gamma|$ and the phase of Γ as functions of frequency separation X at a given receiving point. The results are presented in terms of the normalized parameters C, ζ_0, ζ, etc. The set of values $C = 1.55$, $\zeta_0 = 0.212$, $\zeta = 1.484$ corresponds to ionospheric parameters $L = 50$ km, $l_0 = 330$ m, $f_p = 6$ MHz, $\langle(\Delta N/N_0)^2\rangle^{1/2} = 5\%$, and $z = 350$ km for a wave frequency $f = 125$ MHz. We note that in general, $|\Gamma|$ decreases monotonically as X increases while arg Γ seems to increase with X and for the gaussian spectrum it actually reaches a maximum and then decays. For small X, $|\Gamma|$ is larger for the gaussian spectrum than the case for the power-law spectrum. But as X increases, $|\Gamma|$ decreases faster for the gaussian case. Figure 3 shows the results for similar computations but for $\zeta_0 = 1.698$, corresponding to a slab eight times thicker than that in Figure 2. Because of more scattering, the signal is rapidly decorrelated with the bandwidth as is evident from the figure, becoming nearly uncorrelated when the frequency separation is 20%.

For a given set of ionospheric parameters, it is possible to study the dependence of Γ on the carrier frequency of the signal. Figure 4 shows the results of such computations for $L = 50$ km, $l =$

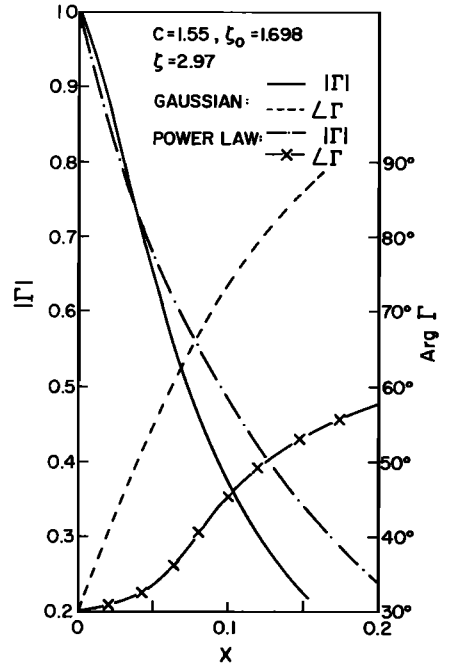

Fig. 3. Same as Figure 2 but for greater slab thickness.

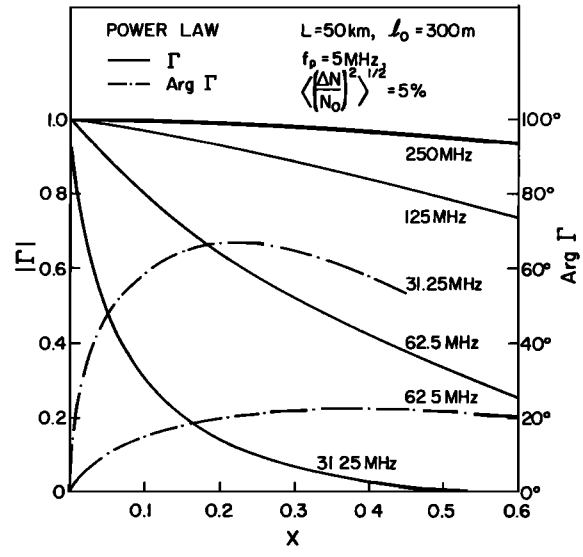

Fig. 4. Amplitude and phase of Γ as functions of frequency separation with carrier frequency as parameter, for power-law spectrum.

300 m, $f_p = 5$ MHz, $\langle(\Delta N/N_0)^2\rangle^{1/2} = 5\%$, and $z = 350$ km. We note that for $f = 250$ MHz, the signal is very well correlated even when $X = 0.6$. As f decreases, the correlation also decreases. This result is consistent with the observation that the fluctuation of the refractive index in the ionosphere is inversely proportional to the square of the wave frequency. We note that for $f = 31.28$ MHz, $|\Gamma|$ becomes sharply peaked as a function of X. The antisymmetric mutual coherence function $\bar{\Gamma}$ is found to depend on X very weakly. However, its value seems to depend on the strength of scattering. Figure 5 shows $|\bar{\Gamma}|$ as a function of carrier frequency for a given set of ionospheric parameters. We see that $|\bar{\Gamma}|$ is very small at lower frequencies and it increases to values comparable to those of $|\Gamma|$ as the frequency increases. This implies that when the wave frequency is low so that the scattering is strong and the slab thickness is large, the variances of the in-phase and the phase-quadrature components of the signal are almost equal and the antisymmetric mutual coherence function is very small. On the other hand, when the scattering is very weak, the variance of the in-phase component dominates. When this is the case, the channel cannot be treated as a symmetric channel [*Bello*, 1971].

In Figures 2-5 we have presented the mutual coherence functions at a fixed receiving position. We wish now to generalize these functions by introducing both the frequency and spatial correlations for the ionospheric scintillation channel. Define the correlation coefficient as

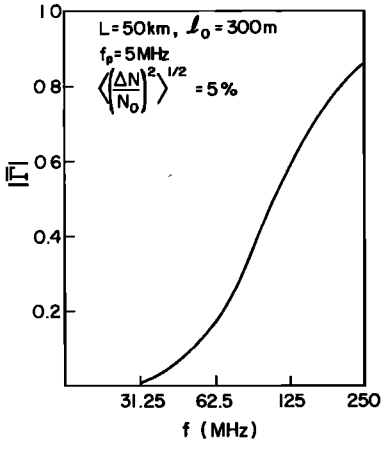

Fig. 5. Amplitude of $\bar{\Gamma}$ as a function of carrier.

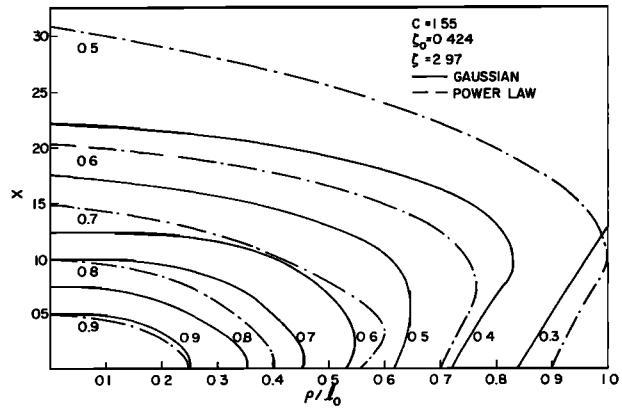

Fig. 6. Contour curves for constant correlation coefficients, plotted in the $X - \rho/l_0$ plane for a given set of ionospheric parameters.

$$C_u = \frac{|\langle(u_1 - \langle u_1\rangle)(u_2^* - \langle u_2^*\rangle)\rangle|}{(\langle|u_1 - \langle u_1\rangle|^2\rangle\langle|u_2 - \langle u_2\rangle|^2\rangle)^{1/2}}$$

$$= \frac{|\Gamma(\vec{\rho}, z, \omega_0, X) - \langle u_1\rangle\langle u_2^*\rangle|}{[(\langle u_1^2\rangle - \langle u_1\rangle^2)(\langle u_2^2\rangle - \langle u_2\rangle^2)]^{1/2}} \tag{33}$$

where [*Liu et al.*, 1974*a*]:

$$\langle u_i\rangle = \exp[-k_i^2 A(0)L/8] \tag{34}$$

and

$$\langle u_i^2\rangle = |\Gamma(0, z, \omega_0, 0)| \tag{35}$$

The correlation coefficient so defined is seen related to the mutual coherence function. Once the mutual coherence is computed, (33) can be used to compute C_u. In Figures 6 and 7 are plotted the constant C_u contours in the $X - (\rho/l_0)$ plane for different

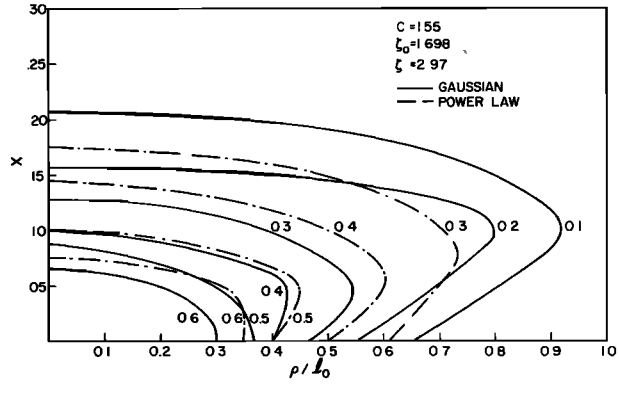

Fig. 7. Same as Figure 6 but for greater slab thickness.

sets of ionospheric parameters. The general shape of the contours is the same in both cases. In Figure 7, the curves are compressed toward the origin, indicating more decorrelation for a given spatial and frequency separation. This is to be expected since the parameters in Figure 7 correspond to a thicker irregularity slab. If one follows a constant C_u contour starting from zero spatial separation, these curves show that as X decreases, in order to maintain the same amount of correlation (or decorrelation), the spatial separation has to increase. This trend continues until the spatial separation reaches a maximum. Beyond this maximum, further decrease of frequency separation results in a decrease in ρ/l_0. This implies that in the neighborhood of this maximum ρ/l_0, for a fixed value of spatial separation, there may exist two values of frequency separation at which C_u has the same value. This result has obvious implications in the study of frequency and/or spatial diversity communication schemes.

To interpret this interesting result, we resort to a rather simple model. As is well known, the scattering process is closely related to the Fresnel filtering effect [*Yeh et al.*, 1975]. It is then reasonable to assume that the degree of frequency and spatial correlation of the signal is proportional to the amount of overlapping Fresnel zones corresponding to the two frequencies at the two spatial points. Since the Fresnel zone is proportional to $1/f^{1/2}$, in the absence of spatial separation, the Fresnel zones at the two frequencies are proportional to $(1 + X)^{-1/2}$ and $(1 - X)^{-1/2}$ respectively. The overlap is therefore the smaller of the two or $P(1 + X)^{-1/2}$ where P is a proportionality constant. Hence as X increases, the frequency correlation decreases as expected. This is true when there is no spatial separation. The situation gets a little bit more complicated when there is spatial separation ρ. Let us refer to Figure 8. The two receivers are at 0 and 0′, separated by a distance ρ. The corresponding Fresnel zones at two frequencies when projected on the ground are indicated by $A'A$ and $B'B$ respectively. From the figure, it is not difficult to write down the overlapping region of the Fresnel zones as

$$(P/2)(1 + X)^{-1/2} - \rho + (P/2)(1 - X)^{-1/2} \cong P - \rho + (3/2)PX^2, \quad \text{for } X \text{ small} \tag{36}$$

We see that in this region the overlap increases as X increases, indicating higher correlation coefficient for larger X. This is essentially the behavior of the contour curves for small X. As X increases further such that

$$(P/2)(1 - X)^{-1/2} - \rho > (P/2)(1 + X)^{-1/2} \tag{37}$$

we see from the figure that under this condition the overlap reduces to $P(1 + X)^{-1/2}$ again, hence, decreasing correlation for increasing X. This simple picture seems to explain qualitatively the behavior of the correlation contour curves.

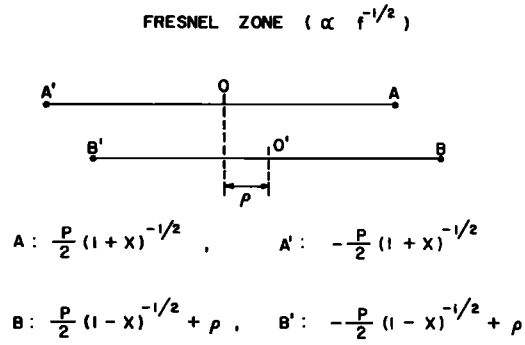

Fig. 8. The overlapping Fresnel zones.

4. CONCLUSIONS

In this paper, the frequency and spatial correlations of transionospheric scintillating radio signals are investigated by using the mutual coherence functions. Equations are derived for the mutual coherence functions taking into account the effects of multiple scattering. The effects of the background ionosphere have also been included, although in the numerical computations the emphasis is on the random scattering. The full equations can be used to model theoretically the transionospheric communication channel including effects on dispersion and stratification as well as scattering.

Numerical results for frequency correlation are presented for cases of strong scattering and large frequency separation. The decorrelation effects of scattering are obviously indicated. Study of both frequency and spatial correlations shows that for a given spatial separation, in order to achieve a given level of decorrelation, there may exist two values of frequency separation. This result turns out to be explainable by using the simple picture of overlapping Fresnel zones.

Acknowledgments. This work was partially supported by the Atmospheric Sciences Section, National Science Foundation, under grant GA-42857.

REFERENCES

Bello, P. A. (1971), A study of the relationship between multipath distortion and wavenumber spectrum of refractive index in radio links, *Proc. IEEE, 59,* 47–75.

Craft, H. D., Jr., and L. H. Westerlund (1972), Scintillation at 4 and 6 GHz caused by the ionosphere, paper presented at the AIAA 10th Aerospace Sciences Meeting, San Diego, California.

Dyson, P. L. (1969), Direct measurements of the size and amplitude of irregularities in the topside ionosphere, *J. Geophys. Res., 74,* 6291–6303.

Dyson, P. L., J. P. McClure, and H. B. Hanson (1974), In-situ measurements of amplitude and scale size characteristics of ionospheric irregularities, *J. Geophys. Res., 79,* 1497–1502.

Erukhimov, L. M., I. G. Zarnitsyna, and P. I. Kirsh (1973), Selective properties and shape of a pulse signal that has passed through a statistically inhomogeneous layer of arbitrary thickness, *Radiophys. Quantum Electron., 16,* 436–441.

Lee, L. C. (1974), Wave propagation in a random medium: A complete set of the moment equations with different wavenumbers, *J. Math. Phys. (NY), 15,* 1431–1435.

Liu, C. H., A. W. Wernik, K. C. Yeh, and M. Y. Youakim (1974*a*), Effects of multiple scattering on scintillation of transionospheric radio signals, *Radio Sci., 9,* 599–607.

Liu, C. H., A. W. Wernik, and K. C. Yeh (1974*b*), Propagation of pulse trains through a random medium, *IEEE Trans. Antennas Propagat., AP-22,* 624–627.

McClure, J. P., and W. B. Hanson (1973), A catalog of ionospheric *F* region irregularity behavior based on OGO 6 retarding potential analyzer data, *J. Geophys. Res., 78,* 7431–7440.

Pope, J. H., and R. B. Fritz (1971), Observations of simultaneous scintillation on VHF and *S*-band satellite transmissions at high latitudes, *Indian J. Pure Appl. Phys., 9,* 593–600.

Rufenach, C. L. (1972), Power-law wavenumber spectrum deduced from ionosperic scintillation observations, *J. Geophys. Res., 77,* 4761–4772.

Sessions, W. B. (1972), Amplitude fading of simultaneous transionospheric *L*-band and VHF signals received at the geomagnetic equator, *Tech. Rep. X-810-72-282,* Goddard Space Flight Center, Greenbelt, Maryland.

Skinner, N. J., R. F. Kelleher, J. B. Hacking, and C. W. Benson (1971), Scintillation fading of signals in the SHF band, *Nature, 232,* 19–21.

Tatarski, V. I. (1971), *The Effects of the Turbulent Atmosphere on Wave Propagation,* 472 pp., National Technical Information Service, Springfield, Va.

Taur, R. R. (1973), Ionospheric scintillation at 4 and 6 GHz, *COMSAT Tech. Rev., 3,* 145–163.

Ulaszek, S. J., C. H. Liu, and K. C. Yeh (1975), Frequency correlation and coherent bandwidth of transionospheric signals, paper 4–4 in *Proc. Symposium on the Effects of the Ionosphere on Space Systems and Communications,* edited by J. M. Goodman, Washington, DC.

Yeh, K. C., and C. H. Liu (1972), *Theory of Ionospheric Waves,* Academic, New York.

Yeh, K. C., C. H. Liu, and M. Y. Youakim (1975), A theoretical study of the ionospheric scintillation behavior caused by multiple scattering, *Radio Sci., 10,* 97–106.